The Radial Evolution of Magnetic Clouds From Helios to Ulysses

Ake Zhao[1,2] , Yuming Wang[3,4] , Hengqiang Feng[2,5] , Long Cheng[3] , Xiaolei Li[3], Qiangwei Cai[5] , Hongbo Li[5] , and Guoqing Zhao[5]

[1] College of Physics and Electric Information, Luoyang Normal University, Luoyang 471934, People's Republic of China; zzukeer@mail.ustc.edu.cn
[2] Henan Key Laboratory of Electromagnetic Transformation and Detection, Luoyang Normal University, Luoyang 471934, People's Republic of China
[3] CAS Key Laboratory of Geospace Environment, Department of Geophysics and Planetary Sciences, University of Science and Technology of China, Hefei, Anhui 230026, People's Republic of China
[4] CAS Center for Excellence in Comparative Planetology, Hefei, People's Republic of China
[5] Institute of Space Physics, Luoyang Normal University, Luoyang 471934, People's Republic of China

Abstract

The evolution of a magnetic cloud (MC) from the inner heliosphere to the outer heliosphere has been investigated for decades. Although many studies have reported on the evolution of MCs, there is no relevant statistical study about the continuous parametric evolution of the flux rope model of the Gold–Hoyle solution for MCs from near the Sun to 5.4 au. Based on the velocity-modified uniform-twist force-free flux rope model, in this study we explore the evolution with heliodistance for some parameters from 139 MCs observed by the Helios, Wind, and Ulysses spacecraft. We find a negative/positive correlation between the central axial field strength/the radius of the cross section and the heliodistance. The angle between the axis of the MC and the Sun–spacecraft line (Θ), the expansion velocity (v_e), and the poloidal velocity (v_p) did not show any evident tendency to increase or decrease with the heliodistance. In addition, the number of turns of the magnetic field lines per unit length winding around the magnetic flux rope, τ, shows a weak decrease with heliodistance. Also, there is an evident negative correlation between τ and the radius of the flux rope, R. The axial magnetic flux (F_z) and the magnetic helicity (H_m) show a tendency to decrease within 1 au, after which they remain almost unchanged until 5.5 au. Furthermore, we do not find any evident difference in the parametric properties of MCs on and outside the ecliptic.

Unified Astronomy Thesaurus concepts: Heliosphere (711); Solar coronal mass ejections (310)

1. Introduction

Coronal mass ejections (CMEs) are large expulsions of magnetic field and plasma structures that erupt from the solar atmosphere. Interplanetary coronal mass ejections (ICMEs) are the counterparts of CMEs that move from the Sun to the outer heliosphere and can induce strong geomagnetic storms when they interact with Earth's atmosphere. Magnetic clouds (MCs) are ICMEs characterized by an enhanced magnetic field strength, large and smooth rotation of the magnetic field vector, low proton beta, and a low proton temperature (Burlaga et al. 1981; Klein & Burlaga 1982). As MCs are responsible for extreme space weather effects when they interact with Earth's atmosphere, their radial evolution has received special attention over the last few decades.

Currently, two methods are used to study the characteristics of the global radial evolution of MCs: radial conjunctions of spacecraft measurements for the same MC and different MC events measured at a different heliocentric distances. The first method is limited to case studies, while the second is based on statistical analysis.

The radial alignments of two or more spacecraft crossed by the same cloud on its way outward represent a unique opportunity to study its actual evolution. However, because of the rarity of such spacecraft conjunctions, only a few MCs have been observed using the first method. Fortunately, some events are still observed by radially aligned spacecraft, and are

important for studying the evolution of MC structure in the heliosphere. For example, Skoug et al. (2000) studied the evolution of electrons as an MC observed by ACE and Ulysses spacecraft. They found the electron temperature and density decreased as the MC expanded from 1 to 5.4 au. Du et al. (2007) studied the evolution of an MC from ACE to Ulysses and found that the MC was expanding while propagating outward, and the axial and poloidal magnetic fluxes were different but of approximately the same order of magnitude. However, the magnetic helicity contained in each flux rope differs significantly; they guessed that this might be caused by underestimation of the area of the flux rope at Ulysses. Rodriguez et al. (2008) analyzed the in situ observation of two MCs at 1 au and at Ulysses. They found that the global magnitudes of magnetic fluxes and helicity were retained well from their solar source to 5 au, and the two events are expanding while propagating outward. Also, Gulisano et al. (2010) analyzed MCs observed by the two Helios spacecraft and discovered that the total solar wind pressure with distance was the main origin of the observed MC expansion rate. However, an MC observed by MESSENGER and STEREO-B between 0.44 and 1.09 au indicated that the cloud's radial width increased by a factor of ∼2.3, and the axial magnetic field strength decreased by a factor of ∼5.3 with the help of force-free fitting (Good et al. 2015). Nakwacki et al. (2011) studied the dynamical evolution of an MC from the Sun to 5.4 au, and found that the flux rope is significantly distorted at 5.4 au. Also, Li et al. (2017) tracked the radial evolution of an interplanetary coronal mass ejection from 1 au by Wind to 5.4 au by Ulysses, and they obtained the evolution of Alfvénic fluctuations and their contribution to local plasma heating. Witasse et al. (2017) investigated the Forbush decreases of an

interplanetary coronal mass ejection observed by STEREO-A, Mars, comet 67P, and Saturn spacecraft. In addition, Good et al. (2018) examined the magnetic field structures of two ICMEs observed by a pair of spacecraft (MESSENGER and STEREO-B) close to radial alignment and found that the magnetic field profiles were similar at different heliocentric distances. Moreover, Wang et al. (2018) reported an MC that was observed sequentially by four spacecraft near Mercury, Venus, Earth, and Mars and found that the axial magnetic flux and helicity of the MC decreased when the MC propagated outward, but the twist increased. This phenomenon may be jointly caused by the "pancaking" effect and "erosion" effect. Also, Kilpua et al. (2019) reported CME–CME interactions during their evolution using in situ observations from almost radially aligned spacecraft at Venus and Earth. For the first time, Telloni et al. (2020) studied the turbulent evolution of the magnetohydrodynamic properties of an MC observed by alignments of Wind and Ulysses spacecraft, which provided compelling evidence of magnetic erosion of the structure.

Statistical research for different MCs measured at different heliocentric distances can also provide us with some hints to obtain the characteristic of the global evolution of MCs. Wang et al. (2005) identified approximately 600 ICMEs from 0.3 to 5.4 au by Helios 1 and 2, Pioneer Venus Orbiter, ACE, and Ulysses. They found that the occurrence rate of ICMEs follows the solar activity cycle. Furthermore, ICMEs expanded as they moved outward because the internal pressure was larger than the external pressure; the ICMEs expanded by a factor of 2.7 in radial width between 1 and 5 au. At the same time, Wang et al. obtained the radial expansion speed of ICMEs: it decreased with distance and was consistent with the Alfvén speed. Based on the fitting results for 130 MCs of the force-free, constant-α flux rope model, Leitner et al. (2007) explored three different approaches to study the evolution of the average central axial field strength, the average diameter, and other parameters with heliospheric distance from 0.3 to 7 au. Du et al. (2010) analyzed the occurrence rate of ICMEs, the interaction of ICMEs with the solar wind, and the magnetic field properties of the ICMEs observed by Ulysses from 1.41 to 5.41 au. Based on fitting with a cylindrically symmetric Gold–Hoyle force-free uniform-twist flux rope configuration, Vršnak et al. (2019) investigated the interplanetary evolution of 11 MCs recorded by at least two radially aligned spacecraft. They found that MCs had a self-similar expansion behavior, and in most individual events the inferred magnetic field decreased much more slowly than expected. Using a modified statistical method and analysis from individual conjunctions of 47 CMEs measured in situ in the inner heliosphere by two or more radially aligned spacecraft (MESSENGER, STEREO, Wind/ ACE), Salman et al. (2020) found an exponential decrease of the axial magnetic field strength in the CME with heliodistance. Recently, with the help of the velocity-modified Gold–Hoyle model, Raghav et al. (2020) investigated the characteristic of 26 MCs observed by the Helios 1 and 2 spacecraft (from 0.3 to 1 au), and found that the expansion speed, poloidal speed, total magnetic helicity, and twist per au of the MC did not depend on the heliospheric distance.

Though there are many case studies and much statistical research on the evolution of MCs, there is no relevant statistical study about the parametric continuous evolution of the flux rope model of the Gold–Hoyle solution for MCs from near the Sun to 5.4 au. In Section 2, the Helios 1 and 2, Wind, and Ulysses spacecraft and the data availability are described. The parametric evolution characteristics of MCs are described in Section 3. In Section 4, a summary and discussion are presented.

2. Spacecraft and Data

2.1. Spacecraft

In this work, the starting point is three lists of events reported by Raghav et al. (2020), Wang et al. (2016), and Du et al. (2010), respectively. The first list contains 26 MCs observed by the Helios 1 and 2 spacecraft (from 0.38 to 0.96 au); the second contains 100 MCs (from Lepping et al. 2006) observed by the Wind spacecraft; the third list contains 77 MCs observed by the Ulysses spacecraft. Helios was a joint German–American deep-space mission to study the main solar processes and solar–terrestrial relationships. Helios 1, launched in 1974 December, reached a perihelion distance of 0.309 au, while Helios 2, launched in 1976 January, reached a perihelion distance of 0.290 au. Helios 2 stopped working in 1980 March, while Helios 1 stopped working after almost 60 months of active life. The scientific goal of the double mission was to investigate the interplanetary matter between the Sun and the Earth's orbit.

The Wind spacecraft was launched on 1994 November 1 and was designed to observe the solar wind approaching Earth. It was placed in a halo orbit around the L1 Lagrange point; hence, the data from the Wind spacecraft have been considered as the data near 1 au.

The purpose of the Ulysses mission was to explore the history of the three-dimensional structure of our whole solar system by spacecraft. After its launch in 1990 October, a gravity assist at Jupiter was employed to change the orbital plane of Ulysses such that it reached high solar latitudes; there, Ulysses completed three pole-to-pole fast scans from 1.3 to 5.4 au and up to 80° heliolatitude. Data provided by Ulysses led to the discovery that the Sun's magnetic field interacts with the solar system in a more complex fashion than previously assumed.

2.2. Data

Helios, Wind, and Ulysses spacecraft provided us with a good opportunity to investigate the whole evolution of MCs from the inner to outer heliosphere and low to high heliolatitude. The MCs studied in this study must have typical flux tube characteristics. Therefore, MCs were obtained and fitted using a model. If the fitting results are not good, the fitting parameters are unreliable and statistical analysis cannot be performed, so we abandon them. Given our data set, we use the velocity-modified uniform-twist force-free flux rope model (Wang et al. 2016) to fit the measurements of the magnetic field and velocity. The time resolution of the fitting data is 5 minutes on average. Because of the lack of plasma velocity data for events 131, 134, 137, 140, and 143 in Table 1 in Du et al. (2010), 72 of 77 MCs measured by Ulysses are fitted. The basic parameters obtained from the fitting are magnetic field strength on the axis of the flux rope (B_0), radius of the cross section of the flux rope (R), and the twist, which is the number of turns per unit length along the flux rope axis (τ). The axial and poloidal magnetic fluxes are calculated from

$$F_z = \int_0^{2\pi} \int_0^R B_z r dr d\varphi = \frac{B_0 l^2}{4\pi n^2} \ln\left(1 + 4\pi^2 n^2 \frac{R^2}{l^2}\right) \quad (1)$$

$$F_\varphi = \int_0^l \int_0^R |B_\varphi| dr dz = \frac{B_0 l^2}{4\pi|n|} \ln\left(1 + 4\pi^2 n^2 \frac{R^2}{l^2}\right) \quad (2)$$

where l is the axial length and n is the number of turns of the field lines winding around the axis from one end of the magnetic flux rope to the other. The total magnetic helicity is

$$H_m = n F_z^2. \quad (3)$$

These events selected should satisfy the following conditions: (1) normalized rms (χ_n) of the difference between the modeled and observed data is less than or equal to 0.5, where χ_n is evaluated from

$$\chi_n = \sqrt{\frac{1}{2N}\sum_{i=1}^{N}\left[\left(\frac{\boldsymbol{B}_i^m - \boldsymbol{B}_i^o}{|\boldsymbol{B}_i^o|}\right)^2 + \left(\frac{\boldsymbol{v}_i^m - \boldsymbol{v}_i^o}{|\boldsymbol{v}_i^o| - v_{\mathrm{ref}}}\right)^2\right]}$$
$$= \sqrt{\frac{1}{2}(\chi_{Bn}^2 + \chi_{vn}^2)} \quad (4)$$

in which the modeled and observed values are marked by superscripts m and o, respectively; N is the number of measurements and v_{ref} is the reference velocity. The equation for χ_n is explained in detail in a previous study (Wang et al. 2015); (2) three quantities related to the twist: the percentage ($\geqslant$ one-third) of the data points falling in the uncertainty range of the modeled twist, the correlation coefficient (cc $\geqslant 0.4$) of the modeled and measured twist, and the confidence level (cl $\geqslant 0.9$) of the correlation under the permutation; (3) the absolute error of the twist is less than or equal to 3.0. If conditions 1, 2 and 3 are satisfied, Q is 1, and if only conditions 1 and 3 are satisfied, Q is 2. The number of MCs with fit quality Q of 1 or 2 is 19 (occupying 73%) measured by Helios, 73 (occupying 73%) measured by Wind, and 47 (occupying 61%) measured by Ulysses. 10 MCs (occupying 38%) having $Q = 1$ are measured by Helios, 47 (occupying 47%) by Wind, and 17 (occupying 22%) by the Ulysses spacecraft. The fitting results for $Q = 1$ or $Q = 2$ are listed in Table 1.

3. Analysis of the Fitting Results

Based on the fitting results, we plot scatter diagrams of parameters for 139 MCs with $Q = 1$ and $Q = 1$ or $Q = 2$, in which the variations are similar to each other. Using the fitting results for $Q = 1$ or $Q = 2$, we investigate the relationship between the fitting parameters and the heliodistance below. The scatter diagram from Helios and Ulysses spacecraft in Figure 1(a) shows a strong negative correlation between the logarithmic magnetic field strength on the axis of the flux rope and the heliodistance, for which the correlation coefficient (cc) is about -0.85 with confidence level (CL) of 0.97. The scatter diagram from the Helios and Ulysses spacecraft in Figure 1(c) shows a strong positive correlation between the logarithmic radius of the cross section of the flux rope and the heliodistance, for which the correlation coefficient is about 0.77, with a confidence level of 0.88.

To further show the variation of these parameters, based on the scatter values, we obtain the median values and error bars for the magnetic field strength on the axis and the radius of the cross section of the flux rope at 0–1 au, 1 au, 1–3 au, 3–5 au, and 5–6 au. Figures 1(b) and (d) show the change of these median values with heliodistance, in which negative/positive

correlations are obvious. The results match well with the fitting results for B_o and R from the flux rope model of the force-free, constant-α Lundquist solution in Leitner et al. (2007).

The parameter Θ is the angle between the MC axis and the Sun–spacecraft line, which could take any value from $0°$ to $90°$. If it is $0°$, it indicates that the spacecraft passes through the leg of the MC; if it is $90°$, it indicates that the spacecraft passes through the head of the MC. The parameter v_e is a constant expansion speed at the boundary of a cross section of the flux rope. The parameter v_p is the poloidal speed of the plasma at the boundary of the flux rope in the direction φ in cylindrical coordinates (r, φ, z), where z is aligned with the central axis (see more details in Wang et al. 2015).

Figures 2(a)–(c) show the changes in Θ, v_e, and v_p with heliodistance, respectively, where there is no evident tendency to increase or decrease. The distributions of the three parameters are shown on the right side of Figures 2(a)–(c), where the median values are about $53°$, 15.89 km s^{-1}, and 9.17 km s^{-1}, meaning that most spacecraft pass through the body of the MCs, and most of the MCs show expansion characteristics during their propagation from the inner heliosphere to the outer heliosphere. Furthermore, plasma poloidal motion is a common phenomenon in MCs.

The number of turns of magnetic field lines per unit length winding around the axis of the magnetic flux rope is given by

$$\tau = \frac{T}{2\pi} \quad (5)$$

where T is the twist of the magnetic field lines in units of radians per unit length. T can also be described by $T = B_\varphi/rB_z$ in local cylindrical coordinates (r, φ, z). The scatter diagram (Figure 3(a)) and median value diagram (Figure 3(b)) show weak negative correlation between τ and the heliodistance, in which the correlation coefficient is -0.34 at a weak confidence level of 0.37, meaning that the magnetic field lines in the MC are slowly unwrapped when they propagate away from the Sun to the outer heliosphere. Figures 3(c) and (d) show the relation between τ and R using scatter plotting and median value plotting, respectively, in which the red dashed line is from the upper limit in Figure 9(a) of Wang et al. (2016), where

$$\tau = \frac{\omega}{2\pi R} \quad (6)$$

and $\omega = 2.0$. If we replace R using our fitting results in Equation (6), and the overestimation factor of 2.5 about τ is also considered, then we plot the blue dashed line, which coincides well with the red line. The negative correlation between τ and R is also evident in median values in Figure 3(d), meaning that a thinner MC has more turns of magnetic field lines, which is consistent with the conclusion in Wang et al. (2016).

If the length of the flux rope's axis is l, then l can be computed from

$$l = \lambda L \quad (7)$$

where L is the heliodistance of the leading part of the MC and λ is the effective length factor. Here λ is set to be $\frac{\pi+2}{2} \pm \frac{\pi-2}{2} \approx 2.57 \pm 0.57$ following Wang et al. (2015). The number of turns of the field lines winding around the axis

Table 1
Fitting Parameters of the MCs Involved in Our Study

		Modeled Parameters																	
N0 (1)	t_0 (2)	Δt (3)	B_0 (4)	R (5)	θ (6)	ϕ (7)	d (8)	τ (9)	v_e (10)	v_p (11)	Θ (12)	F_z (×10^{21}) (13)	F_p (×10^{21}) (14)	H_m (×10^{42}) (15)	χ_n (16)	Long, (17)	Lat, (18)	Dist, (19)	Q (20)
1	1978/04/16 18:36	6.60	84	0.09	−30	101	0.89	$-3.0^{+0.5}_{-0.4}$	58	80	80	2.17 ± 0.29	6.74 ± 1.63	−14.61 ± 5.47	0.12	138.7	−4.8	0.42	2
2	1979/05/28 23:24	12.24	83	0.06	−8	128	−0.34	$-2.2^{+1.0}_{-1.0}$	0	−23	52	1.70 ± 0.40	4.21 ± 1.99	−7.16 ± 5.05	0.33	262.9	7.2	0.43	1
3	1981/05/26 02:16	29.16	50	0.16	59	137	0.25	$-0.9^{+0.3}_{-0.3}$	69	13	67	6.26 ± 0.96	7.00 ± 2.61	−43.80 ± 23.10	0.36	93.4	−7.2	0.47	1
4	1977/04/05 18:18	3.54	44	0.02	30	53	−0.30	$0.3^{+1.0}_{-1.0}$	−6	−16	58	0.09 ± 0.00	0.03 ± 0.11	0.00 ± 0.01	0.23	124.3	−6	0.47	2
5	1980/06/20 02:24	14.40	52	0.06	23	229	−0.48	$-3.0^{+1.5}_{-1.5}$	49	−1	52	0.92 ± 0.32	3.80 ± 1.42	−3.49 ± 2.52)	0.30	287.7	6.9	0.53	1
6	1978/11/29 05:45	5.04	62	0.05	9	315	−0.77	$2.9^{+2.2}_{-2.2}$	14	−17	45	0.80 ± 0.32	0.31 ± 1.98	2.66 ± 2.65	0.36	291.1	6.8	0.55	1
7	1997/03/17 01:48	4.20	14	0.05	23	316	−0.96	$-0.2^{+0.4}_{-0.4}$	7	−3	48	0.27 ± 0.00	0.08 ± 0.19	0.02 ± 0.05	0.15	69.9	−6.8	0.6	2
8	1981/05/11 15:00	13.80	155	0.14	−7	75	−0.44	$-5.4^{+0.7}_{-0.7}$	232	0	75	2.96 ± 0.51	27.16 ± 7.35	−80.36 ± 35.63	0.39	60.1	−6.3	0.66	1
9	1979/04/03 03:50	13.92	57	0.03	0	212	0.42	$5.5^{+1.2}_{-1.3}$	7	−36	32	0.27 ± 0.04	2.61 ± 0.81	0.71 ± 0.32	0.20	91.8	−7.2	0.67	1
10	1977/12/01 14:09	8.40	30	0.04	0	135	−0.65	$-4.3^{+1.1}_{-1.4}$	20	−36	45	0.24 ± 0.05	1.97 ± 0.67	−0.47 ± 0.26	0.26	318.5	4.8	0.75	2
11	1981/04/27 08:52	3.00	34	0.02	−60	315	0.10	$-2.4^{+1.4}_{-1.4}$	0	16	69	0.08 ± 0.00	0.40 ± 0.32	−0.03 ± 0.03	0.22	41.8	−4.8	0.79	1
12	1981/01/27 18:00	7.56	18	0.05	38	30	−0.37	$0.2^{+0.3}_{-0.3}$	21	−52	46	0.28 ± 0.00	0.10 ± 0.20	0.03 ± 0.06	0.19	330.9	3.5	0.85	2
13	1978/12/24 14:24	11.16	23	0.05	−39	39	0.72	$-4.6^{+0.6}_{-0.7}$	−1	−18	52	0.25 ± 0.03	2.48 ± 0.60	−0.61 ± 0.23	0.24	8.5	−1.1	0.85	1
14	1975/11/17 11:02	6.84	12	0.02	9	60	−0.06	$-0.5^{+1.8}_{-1.8}$	1	−7	60	0.05 ± 0.00	0.06 ± 0.21	−0.00 ± 0.01	0.15	334.5	3.1	0.87	2
15	1981/04/14 04:12	20.76	9	0.10	16	327	−0.44	$0.0^{+0.2}_{-0.2}$	56	−1	36	0.61 ± 0.00	0.01 ± 0.27	−0.01 ± 0.16	0.19	29.2	−3.5	0.89	2
16	1979/03/03 09:57	6.72	24	0.04	30	30	0.37	$-1.8^{+0.6}_{-0.6}$	−14	−2	41	0.20 ± 0.01	0.87 ± 0.45	−0.17 ± 0.10	0.20	19.3	−2.4	0.94	1
17	1977/01/29 12:18	8.10	26	0.10	74	68	−0.89	$0.3^{+0.1}_{-0.1}$	71	−14	84	1.99 ± 0.02	1.48 ± 0.73	2.9 ± 1.5	0.11	17.6	−2.2	0.95	2
18	1978/01/06 01:26	5.46	11	0.04	0	240	−0.35	$3.0^{+0.5}_{-0.4}$	15	0	60	0.08 ± 0.00	0.61 ± 0.20	0.05 ± 0.02	0.38	24.4	−3	0.95	1
19	1978/02/16 02:38	30.36	18	0.14	−18	315	−0.47	$2.2^{+0.2}_{-0.2}$	57	−1	47	1.01 ± 0.10	5.55 ± 1.24	5.60 ± 1.80	0.33	53.1	−5.8	0.95	2
20	1995/02/08 05:48	19.00	13	0.08	−7	48	0.35	$-2.7^{+1.0}_{-1.1}$	15	6	49	0.31 ± 0.09	2.17 ± 0.71	−0.67 ± 0.41	0.3				1
21	1995/04/03 07:48	27.00	10	0.10	8	122	−0.47	$1.5^{+0.3}_{-0.3}$	16	−19	57	0.49 ± 0.05	1.88 ± 0.61	0.91 ± 0.40	0.28				1
22	1995/08/22 21:18	22.00	10	0.08	−36	232	0.12	$1.7^{+0.7}_{-0.7}$	13	3	61	0.36 ± 0.08	1.54 ± 0.69	0.55 ± 0.36	0.31				1
23	1995/12/16 05:18	17.00	11	0.05	5	21	0.76	$-1.8^{+0.5}_{-0.6}$	17	10	22	0.17 ± 0.01	0.76 ± 0.35	−0.13 ± 0.07	0.4				1
24	1996/05/27 15:18	40.00	19	0.17	4	54	0.59	$-2.6^{+0.8}_{-0.7}$	14	−7	54	1.02 ± 0.35	6.84 ± 1.86	−6.97 ± 4.31	0.36				1
25	1996/07/01 17:18	17.00	14	0.07	6	75	0.28	$-4.2^{+1.2}_{-1.2}$	13	9	75	0.22 ± 0.06	2.37 ± 0.54	−0.51 ± 0.26	0.38				1
26	1996/08/07 12:18	22.50	7	0.09	−40	299	0.36	$1.7^{+0.5}_{-0.5}$	0	3	67	0.27 ± 0.04	1.19 ± 0.41	0.32 ± 0.16	0.40				1
27	1996/12/24 02:48	32.50	20	0.15	30	60	−0.52	$3.1^{+0.8}_{-0.8}$	29	−7	64	0.82 ± 0.25	6.57 ± 1.78	5.36 ± 3.06	0.32				1
28	1997/01/10 05:18	21.00	37	0.11	−9	299	−0.49	$5.4^{+3.0}_{-2.8}$	6	0	60	0.60 ± 0.43	8.31 ± 3.25	4.97 ± 5.51	0.28				1
29	1997/02/10 03:24	15.00	7	0.08	−60	344	0.49	$0.0^{+0.2}_{-0.2}$	18	24	61	0.36 ± 0.00	0.01 ± 0.18	0.00 ± 0.07	0.27				2
30	1997/04/21 14:30	40.00	11	0.16	32	299	0.23	$1.3^{+1.1}_{-1.1}$	10	4	65	1.17 ± 0.77	3.85 ± 1.75	4.48 ± 4.98	0.45				1
31	1997/05/15 09:06	16.00	19	0.06	−16	134	−0.05	$-3.3^{+1.0}_{-1.0}$	−7	−5	47	0.29 ± 0.07	2.52 ± 0.78	−0.74 ± 0.39	0.39				1
32	1997/06/09 02:18	21.00	21	0.06	−8	210	0.59	$6.3^{+1.8}_{-1.7}$	7	9	31	0.18 ± 0.05	2.86 ± 0.72	0.51 ± 0.29	0.34				1
33	1997/06/19 05:06	10.80	13	0.05	−58	314	−0.48	$7.2^{+1.4}_{-1.4}$	10	11	68	0.08 ± 0.02	1.45 ± 0.33	0.11 ± 0.05	0.25				1
34	1997/09/22 00:48	16.50	17	0.08	59	134	0.13	$-2.2^{+0.3}_{-0.3}$	50	8	68	0.49 ± 0.04	2.72 ± 0.75	−1.34 ± 0.47	0.12				1
35	1997/10/01 16:18	30.50	10	0.16	60	139	−0.24	$-0.7^{+0.2}_{-0.2}$	9	8	67	1.33 ± 0.16	2.46 ± 1.07	−3.27 ± 1.80	0.29				1
36	1997/10/10 23:48	25.00	13	0.10	−7	232	−0.17	$2.5^{+1.2}_{-1.2}$	25	−11	52	0.46 ± 0.19	3.02 ± 0.87	1.40 ± 0.98	0.32				1
37	1997/11/07/15:48	12.50	17	0.05	30	224	0.10	$2.7^{+0.6}_{-0.6}$	7	−9	52	0.23 ± 0.02	1.60 ± 0.55	0.36 ± 0.16	0.13				1
38	1997/11/08 04:54	10.00	22	0.05	56	8	−0.61	$6.0^{+2.0}_{-2.0}$	8	19	56	0.16 ± 0.05	2.41 ± 0.59	0.38 ± 0.21	0.30				1
39	1997/11/22 15:48	20.50	31	0.07	22	187	0.60	$-6.2^{+2.2}_{-2.1}$	16	12	23	0.29 ± 0.12	4.60 ± 1.26	−1.33 ± 0.90	0.47				2
40	1998/01/07 03:18	29.00	40	0.14	56	134	−0.47	$-4.3^{+0.8}_{-0.8}$	27	−1	67	1.05 ± 0.25	11.66 ± 3.26	−12.27 ± 6.34	0.23				1
41	1998/02/04 04:30	42.00	13	0.04	0	7	−0.36	$-6.1^{+2.2}_{-2.3}$	13	−15	7	0.07 ± 0.02	1.13 ± 0.33	−0.08 ± 0.05	0.35				1

Table 1
(Continued)

No (1)	t_0 (2)	Δt (3)	B_0 (4)	R (5)	θ (6)	ϕ (7)	d (8)	τ (9)	v_e (10)	v_p (11)	Θ (12)	F_z ($\times 10^{21}$) (13)	F_p ($\times 10^{21}$) (14)	H_m ($\times 10^{42}$) (15)	χ_n (16)	Long, (17)	Lat, (18)	Dist, (19)	Q (20)
42	1998/03/04 14:18	40.00	26	0.14	14	50	0.44	$4.4^{+1.1}_{-1.1}$	9	0	51	0.66 ± 0.21	7.48 ± 2.26	-4.91 ± 3.08	0.26				1
43	1998/06/02 10:36	5.30	14	0.02	10	44	0.48	$-10.0^{+2.1}_{-2.4}$	21	18	45	0.02 ± 0.00	0.60 ± 0.18	-0.01 ± 0.01	0.18				1
44	1998/06/24 16:48	29.00	14	0.15	45	120	0.24	$-1.5^{+0.4}_{-0.4}$	22	8	69	1.28 ± 0.27	4.92 ∓ 1.35	-6.32 ∓ 3.03	0.28				1
45	1998/08/20 10:18	33.00	22	0.11	-7	232	0.34	$3.7^{+2.2}_{-1.9}$	17	12	52	0.56 ± 0.38	5.35 ± 1.63	3.01 ± 2.93	0.40				1
46	1998/11/08 23:48	25.20	34	0.13	-45	159	0.51	$4.5^{+1.1}_{-1.1}$	52	-7	48	0.78 ± 0.24	8.97 ± 2.61	7.01 ± 4.23	0.34				1
47	1999/02/18 14:18	22.00	9	0.14	-32	312	-0.10	$-0.8^{+0.2}_{-0.2}$	106	0	54	1.10 ± 0.08	2.29 ± 0.79	-2.51 ± 1.06	0.37				1
48	1999/04/16 20:18	25.00	24	0.11	-37	127	0.10	$-2.8^{+1.0}_{-1.0}$	30	3	61	0.84 ± 0.29	6.02 ± 1.35	-5.03 ± 2.87	0.39				1
49	1999/08/09 10:48	29.00	19	0.12	60	15	0.57	$-3.5^{+2.3}_{-2.3}$	-3	0	61	0.59 ± 0.44	5.35 ± 1.78	-3.16 ± 3.43	0.32				1
50	1999/09/21 21:06	8.00	13	0.03	-4	132	-0.03	$-7.0^{+1.9}_{-1.9}$	-7	3	47	0.04 ± 0.01	0.70 ± 0.22	-0.03 ± 0.01	0.24				1
51	2000/02/21 09:48	27.50	34	0.12	54	330	-0.43	$4.9^{+2.8}_{-2.5}$	33	-3	59	0.68 ± 0.51	8.43 ± 0.37	5.70 ± 6.61	0.32				1
52	2000/07/28 21:06	13.00	14	0.04	-7	337	0.50	$-3.2^{+1.8}_{-2.0}$	11	-4	23	0.11 ± 0.03	0.88 ± 0.54	-0.09 ± 0.08	0.29				2
53	2000/08/01 00;06	15.80	17	0.03	2	194	0.87	$-8.7^{+0.9}_{-1.0}$	8	-71	14	0.05 ± 0.00	1.00 ∓ 0.25	-0.05 ± 0.02	0.21				2
54	2000/08/12 06:06	23.00	35	0.13	7	52	0.37	$-2.3^{+1.2}_{-1.2}$	59	-19	52	1.75 ± 0.90	10.39 ± 2.53	-18.22 ± 13.74	0.47				1
55	2000/10/03 17:06	21.00	20	0.09	34	60	0.18	$3.1^{+1.1}_{-1.0}$	15	-18	66	0.54 ± 0.18	4.28 ± 1.02	2.29 ± 1.34	0.27				1
56	2000/10/13 18:24	22.50	12	0.10	-38	125	-0.07	$1.6^{+0.8}_{-0.8}$	0	18	63	0.57 ± 0.16	2.30 ∓ 1.09	1.32 ± 0.99	0.20				1
57	2000/10/28 23:18	25.00	15	0.11	-23	119	-0.38	$-1.2^{+0.1}_{-0.1}$	38	-11	63	0.96 ± 0.02	2.88 ± 0.72	-2.76 ± 0.75	0.28				1
58	2001/04/04 20:54	11.50	22	0.14	-23	60	0.82	$2.7^{+1.3}_{-1.3}$	67	-64	63	1.03 ± 0.57	7.05 ± 1.94	7.26 ± 6.01	0.29				2
59	2001/04/12 07:54	10.00	61	0.08	8	198	0.87	$8.9^{+2.4}_{-2.2}$	95	54	20	0.40 ± 0.15	9.12 ± 2.91	3.66 ± 2.52	0.31				1
60	2001/04/22 00:54	24.50	17	0.10	-45	308	0.32	$2.8^{+0.2}_{-0.2}$	27	0	64	0.52 ± 0.04	3.78 ± 0.86	-1.97 ± 0.60	0.19				1
61	2001/05/28 11:54	22.50	14	0.08	-14	30	0.52	$-3.3^{+0.8}_{-0.8}$	-5	4	33	0.31 ± 0.07	2.57 ± 0.64	-0.79 ± 0.38	0.23				1
62	2001/10/31 21:18	37.00	20	0.14	-7	119	-0.27	$-4.1^{+0.5}_{-0.6}$	22	-1	60	0.54 ± 0.09	5.76 ± 1.50	-3.13 ± 1.35	0.31				2
63	2002/03/19 22:54	16.50	16	0.06	12	44	-0.35	$2.2^{+0.2}_{-0.2}$	-7	-23	46	0.27 ± 0.01	1.51 ± 0.41	0.40 ± 0.12	0.19				1
64	2002/03/24 03:48	13.00	28	0.19	21	224	0.47	$2.6^{+1.1}_{-1.1}$	5	6	48	1.76 ± 0.92	11.62 ∓ 3.72	20.48 ± 17.22	0.42				1
65	2002/04/20 11:48	29.00	25	0.21	-14	53	0.71	$-3.2^{+2.1}_{-2.1}$	74	31	54	1.30 ± 1.17	10.51 ± 4.82	-13.61 ± 18.54	0.27				2
66	2002/05/19 03:54	19.50	23	0.25	-3	104	0.92	$-1.4^{+0.1}_{-0.1}$	75	-21	75	3.54 ± 0.20	12.87 ± 2.90	-45.62 ± 12.85	0.28				2
67	2002/08/02 07:24	13.70	13	0.07	-11	240	0.06	$-1.7^{+0.4}_{-0.4}$	18	-11	61	0.35 ± 0.03	1.49 ± 0.56	-0.52 ± 0.24	0.11				1
68	2002/09/03 00:18	18.50	13	0.06	34	203	0.45	$3.7^{+2.8}_{-2.9}$	-19	15	40	0.84 ± 0.12	1.82 ± 0.71	0.35 ± 0.36	0.47				1
69	2003/06/17 17:48	14.50	16	0.08	-13	315	0.63	$-2.9^{+0.6}_{-0.6}$	-35	25	46	0.38 ± 0.06	2.86 ± 0.73	-1.08 ± 0.45	0.36				1
70	2003/08/18 11:36	16.80	14	0.09	-60	314	0.01	$1.0^{+0.5}_{-0.5}$	-21	15	69	0.71 ± 0.09	1.87 ± 1.01	1.32 ± 0.88	0.31				1
71	2003/11/20 10:48	15.50	49	0.10	-54	146	0.12	$4.9^{+1.7}_{-1.6}$	81	6	60	0.81 ± 0.34	10.29 ± 3.00	8.37 ± 5.94	0.37				1
72	2004/04/04 02:48	36.00	17	0.15	52	7	-0.13	$-1.2^{+0.3}_{-0.3}$	12	-14	53	1.74 ± 0.26	5.48 ± 1.63	-9.54 ± 4.27	0.35				1
73	2004/11/09 20:54	6.50	84	0.04	18	327	0.51	$-13.0^{+2.5}_{-2.5}$	24	3	36	0.23 ± 0.06	7.72 ± 2.15	-1.79 ± 0.94	0.30				1
74	2004/11/10 03:36	7.50	38	0.06	-48	15	0.59	$-4.5^{+1.4}_{-1.3}$	67	-10	50	0.47 ± 0.14	5.43 ± 1.34	-2.57 ± 1.38	0.19				1
75	2005/05/20 07:18	22.00	14	0.11	57	314	0.10	$-3.3^{+2.0}_{-2.0}$	0	4	67	0.43 ± 0.29	3.68 ± 1.04	-1.58 ± 1.52	0.46				1
76	2005/06/12 15:36	15.50	31	0.06	-22	164	-0.77	$-6.5^{+1.9}_{-2.3}$	20	17	27	0.24 ± 0.09	3.99 ± 1.00	-0.95 ± 0.61	0.22				2
77	2005/07/17 15:18	12.50	14	0.06	-29	60	0.16	$4.3^{+1.0}_{-1.0}$	32	1	64	0.17 ± 0.04	1.90 ± 0.48	0.33 ± 0.15	0.27				1
78	2006/02/05 19:06	18.00	10	0.07	-34	119	0.19	$2.9^{+2.5}_{-2.2}$	21	5	65	0.19 ± 0.12	1.45 ± 0.67	0.28 ± 0.30	0.45				1
79	2006/04/13 20:36	13.30	20	0.07	-6	299	0.22	$-2.5^{+0.9}_{-0.9}$	10	-10	60	0.46 ± 0.11	2.96 ± 1.06	-1.37 ± 0.80	0.22				1
80	2006/08/30 21:06	17.80	10	0.08	-6	299	0.41	$-3.3^{+0.4}_{-0.4}$	19	-12	60	0.23 ± 0.03	1.93 ± 0.45	-0.44 ± 0.16	0.28				1
81	2007/01/14 14:06	16.80	14	0.05	5	337	0.46	$-3.7^{+0.8}_{-0.8}$	-20	0	23	0.14 ± 0.02	1.38 ± 0.42	-0.20 ± 0.09	0.25				1
82	2007/05/21 22:54	14.70	13	0.05	30	12	-0.13	$6.4^{+2.0}_{-1.9}$	18	-7	32	0.09 ± 0.03	1.43 ± 0.33	0.12 ± 0.07	0.35				1

Table 1
(Continued)

		Modeled Parameters																	
N0 (1)	t_0 (2)	Δt (3)	B_0 (4)	R (5)	θ (6)	ϕ (7)	d (8)	τ (9)	v_e (10)	v_p (11)	Θ (12)	F_z (×10²¹) (13)	F_p (×10²¹) (14)	H_m (×10⁴²) (15)	χ_n (16)	Long, (17)	Lat, (18)	Dist, (19)	Q (20)
83	2007/12/25 15:42	15.10	3	0.06	5	240	−0.33	$-1.1^{+0.3}_{-0.2}$	13	4	60	0.07 ± 0.00	0.18 ± 0.08	−0.01 ± 0.01	0.35				2
84	2008/12/17 03:06	11.30	11	0.04	−5	224	−0.61	$-4.6^{+1.5}_{-1.6}$	19	2	44	0.08 ± 0.02	0.93 ± 0.31	−0.07 ± 0.04	0.19				1
85	2009/01/02 06:06	9.00	6	0.03	7	139	−0.24	$0.9^{+1.3}_{-1.3}$	0	−6	41	0.05 ± 0.00	0.10 ± 0.18	0.01 ± 0.01	0.26				1
86	2009/02/04 00:06	10.80	14	0.04	4	46	−0.58	$5.6^{+2.1}_{-1.9}$	19	−5	46	0.09 ± 0.02	1.25 ± 0.37	0.11 ± 0.06	0.32				1
87	2009/03/12 00:42	21.00	14	0.09	37	139	0.39	$3.6^{+1.2}_{-1.1}$	−27	6	52	0.32 ± 0.11	2.97 ± 0.67	0.96 ± 0.55	0.47				1
88	2009/06/27 15;18	27.00	12	0.10	45	150	0.18	$7.3^{+1.9}_{-1.9}$	10	7	52	0.13 ± 0.04	2.35 ± 0.76	0.29 ± 0.20	0.48				1
89	2009/09/10 10:24	6.00	7	0.02	34	119	0.50	$9.1^{+1.8}_{-1.9}$	5	2	65	0.02 ± 0.00	0.35 ± 0.10	0.01 ± 0.00	0.20				1
90	2009/09/30 07:54	9.00	9	0.03	29	314	0.25	$-4.4^{+1.8}_{-1.7}$	10	5	52	0.05 ± 0.01	0.51 ± 0.22	−0.02 ± 0.01	0.24				1
91	2009/10/29 05:12	17.60	10	0.07	7	230	−0.46	$-1.8^{+0.4}_{-0.4}$	−20	−5	51	0.27 ∓ 0.03	1.27 ∓ 0.46	−0.34 ∓ 0.16	0.29				1
92	2009/12/12 19:48	33.50	8	0.10	−7	134	0.59	$2.3^{+0.2}_{-0.2}$	13	−1	45	0.28 ± 0.02	1.70 ± 0.41	0.48 ± 0.15	0.35				2
93	1991/03/05 04:04	52.00	5	0.24	−41	227	−0.23	$-1.6^{+0.4}_{-0.4}$	30	5	59	0.69 ± 0.19	6.65 ± 1.66	−4.62 ± 2.44	0.33	47.0	−3.4	2.28	1
94	1991/03/16 04:04	56.00	7	0.27	−9	60	−0.12	$1.1^{+0.2}_{0.2}$	50	−10	60	1.56 ± 0.22	10.44 ± 2.38	16.32 ± 5.99	0.26	49.6	−3.7	2.40	2
95	1991/11/17 19:55	50.00	1	0.30	3	59	−0.16	$0.5^{+0.0}_{-0.0}$	15	−1	59	0.60 ± 0.01	3.39 ± 0.82	2.03 ± 0.53	0.26	78.1	−5.8	4.73	2
96	1992/01/12 00:57	35.00	1	0.24	3	60	0.47	$-0.2^{+0.1}_{-0.0}$	8	−12	60	0.46 ± 0.03	1.39 ± 0.95	−0.64 ± 0.48	0.36	81.1	−6.0	5.17	1
97	1992/07/16 07:55	84.00	3	0.42	−52	38	−0.55	$2.4^{+1.4}_{-1.4}$	5	25	61	0.38 ± 0.34	12.36 ± 6.30	4.72 ± 6.65	0.35	83.6	−14.0	5.32	1
98	1992/08/05 17:02	102.00	2	0.60	−45	321	0.53	$-1.1^{+0.2}_{-0.2}$	25	−2	56	0.99 ± 0.24	14.42 ± 4.09	−14.21 ± 7.46	0.29	83.8	−15.0	5.30	1
99	1993/06/09 18:57	79.00	1	0.37	−20	25	0.30	$-0.9^{+0.0}_{-0.0}$	−8	12	31	0.53 ± 0.02	5.51 ± 1.23	−2.90 ± 0.73	0.27	87.4	−32.4	4.65	2
100	1994/02/10 05:02	10.00	2	0.29	−13	317	−0.98	$0.6^{+0.1}_{-0.0}$	−13	3	44	0.85 ∓ 0.04	4.77 ± 1.21	4.06 ± 1.22	0.08	94.1	−52.4	3.63	2
101	1995/02/03 11:02	22.00	9	0.15	−41	15	−0.45	$-3.3^{+0.7}_{-0.7}$	21	22	43	0.33 ± 0.09	3.94 ± 1.06	−1.31 ± 0.70	0.35	257.0	−22.4	1.41	1
102	1996/10/14 13:55	164.00	1	0.25	−7	8	0.21	$1.7^{+0.3}_{-0.3}$	−2	6	10	0.09 ± 0.02	1.76 ± 0.44	0.17 ± 0.08	0.50	76.6	24.3	4.45	2
103	1997/08/16 04:04	74.00	3	0.28	37	315	−0.3	$2.4^{+0.3}_{-0.2}$	11	7	55	0.28 ± 0.04	9.14 ± 2.36	2.59 ± 0.98	0.39	80.0	6.1	5.22	2
104	1997/08/30 06:00	11.00	4	0.08	−35	152	−0.91	$-3.3^{+0.1}_{-0.1}$	17	34	44	0.08 ± 0.00	3.58 ± 0.81	−0.28 ± 0.07	0.18	80.2	5.3	5.25	2
105	1997/10/29 00:57	31.00	2	0.16	28	135	−0.71	$-1.2^{+0.1}_{-0.1}$	0	−11	51	0.21 ± 0.01	3.34 ± 0.86	−0.71 ± 0.23	0.38	80.7	2.3	5.32	1
106	1998/03/23 13:55	110.00	2	0.34	7	158	−0.75	$-1.6^{+0.0}_{-0.0}$	−56	−35	23	0.31 ± 0.01	6.62 ± 1.52	−2.03 ± 0.53	0.41	81.9	−4.9	5.41	2
107	1998/04/01 00:57	96.00	0	0.45	−10	225	0.72	$0.1^{+0.0}_{-0.0}$	37	−3	46	0.57 ± 0.01	1.10 ± 0.42	0.63 ± 0.25	0.48	82.0	−5.3	5.41	2
108	1998/06/18 10:04	95.00	2	0.46	54	325	−0.17	$0.9^{+0.1}_{-0.1}$	24	−9	61	0.98 ± 0.02	12.31 ± 2.93	12.01 ± 4.29	0.37	82.7	−9.1	5.40	2
109	1998/07/10 05:02	172.00	0	2.14	8	277	0.89	$0.0^{+0.0}_{-0.0}$	55	17	83	13.28 ± 0.06	2.36 ± 0.87	31.29 ± 11.69	0.39	82.9	−10.2	5.39	2
110	1998/09/17 18:00	81.00	2	0.30	56	195	0.26	$3.2^{+0.7}_{-0.7}$	23	−1	57	0.14 ± 0.04	5.97 ± 1.93	0.81 ± 0.53	0.39	83.5	−13.6	5.34	1
111	1998/10/10 06:57	123.00	2	0.46	−48	2	−0.43	$0.8^{+0.1}_{-0.1}$	24	14	48	0.74 ± 0.06	8.50 ± 1.96	6.32 ± 1.97	0.30	83.7	−14.7	5.31	2
112	1999/03/03 22:04	46.00	4	0.23	41	306	0.21	$-1.5^{+0.4}_{-0.4}$	25	4	63	0.53 ± 0.16	10.45 ± 2.54	−5.49 ± 3.05	0.31	85.2	−22.3	5.09	1
113	1999/06/12 12:00	59.00	2	0.33	55	218	0.50	$1.2^{+0.1}_{-0.1}$	17	−2	63	0.58 ± 0.05	8.83 ± 2.05	5.12 ± 1.66	0.35	86.4	−28.1	4.86	2
114	1999/10/16 03:07	18.00	3	0.12	−60	33	−0.74	$4.3^{+0.3}_{-0.3}$	2	−3	65	0.08 ± 0.01	4.03 ± 0.98	0.33 ± 0.11	0.38	88.4	−36.2	4.46	2
115	2000/08/10 11:02	45.00	2	0.22	−35	307	0.20	$-1.3^{+0.2}_{-0.2}$	23	−3	60	0.25 ± 0.04	2.64 ± 0.60	−0.67 ± 0.25	0.33	103.9	−65.9	3.01	2
116	2000/12/06 10:04	59.00	3	0.20	−8	225	0.35	$2.0^{+0.5}_{-0.5}$	62	6	45	0.30 ± 0.08	3.43 ± 0.87	1.02 ± 0.54	0.38	190.3	−79.6	2.22	2
117	2001/03/19 09:07	13.00	2	0.05	45	309	0.15	$-0.8^{+1.4}_{-1.5}$	68	6	63	0.05 ± 0.01	0.16 ± 0.29	−0.01 ± 0.02	0.42	252.3	−41.3	1.53	2
118	2001/04/11 05:02	21.00	14	0.15	5	120	−0.58	$-3.6^{+1.2}_{-1.3}$	106	30	60	0.48 ± 0.21	6.43 ± 2.04	−3.09 ± 2.36	0.40	256.1	−26.5	1.43	1
119	2001/05/11 09:07	25.00	13	0.16	−48	210	0.61	$-4.3^{+1.8}_{-1.9}$	43	0	54	0.37 ± 0.22	5.48 ± 2.10	−2.01 ± 1.96	0.43	260.4	−3.9	1.35	2
120	2001/06/07 18:57	27.00	9	0.12	38	323	0.61	$5.4^{+1.6}_{-1.5}$	−7	−9	51	0.15 ± 0.06	2.75 ± 0.88	0.40 ± 0.28	0.33	264.3	17.7	1.35	1
121	2001/07/23 11:02	18.00	7	0.11	12	120	0.68	$0.9^{+0.1}_{-0.1}$	14	13	61	0.45 ± 0.01	1.54 ∓ 0.47	0.70 ± 0.23	0.15	273.0	50.1	1.50	1
122	2001/08/24 13:55	8.00	18	0.05	−8	30	−0.81	$7.4^{+1.3}_{-1.4}$	7	5	31	0.10 ± 40.02	3.36 ± 0.78	0.35 ± 0.15	0.19	285.6	67.3	1.69	1
123	2001/09/28 12:00	27.00	2	0.10	0	12	0.87	$-0.01^{+0.1}_{-0.1}$	−48	13	12	0.12 ± 0.00	0.03 ± 0.09	−0.00 ± 0.01	0.35	324.2	79.0	1.92	2

Table 1
(Continued)

		Modeled Parameters																	
N0 (1)	t_0 (2)	Δt (3)	B_0 (4)	R (5)	θ (6)	ϕ (7)	d (8)	τ (9)	v_e (10)	v_p (11)	Θ (12)	F_z ($\times 10^{21}$) (13)	F_p ($\times 10^{21}$) (14)	H_m ($\times 10^{42}$) (15)	χ_n (16)	Long, (17)	Lat, (18)	Dist, (19)	Q (20)
124	2001/11/14 12:57	25.00	4	0.18	22	60	0.35	$-2.0^{+0.1}_{-0.1}$	12	11	62	0.32 ± 0.02	3.72 ± 0.85	-1.20 ± 0.36	0.32	39.1	75.5	2.26	2
125	2002/01/18 00:57	34.00	3	0.19	7	128	-0.45	$-1.4^{+0.5}_{-0.4}$	1	-12	52	0.39 ± 0.11	3.73 ± 0.99	-1.46 ± 0.81	0.41	61.8	62.3	2.70	2
126	2002/02/11 17:02	24.00	3	0.13	15	126	0.19	$1.1^{+0.3}_{-0.4}$	25	-7	55	0.29 ± 0.05	2.24 ± 0.90	0.65 ± 0.36	0.50	65.0	58.0	2.86	1
127	2002/05/05 06:00	36.00	2	0.17	6	55	-0.63	$1.4^{+0.1}_{-0.1}$	48	7	55	0.25 ± 0.02	3.02 ± 0.71	0.74 ± 0.22	0.34	70.7	46.1	3.36	2
128	2002/06/13 19:55	156.00	3	0.86	-22	225	-0.18	$-0.6^{+0.0}_{-0.0}$	31	14	49	4.24 ± 0.32	23.08 ± 5.47	-97.89 ± 30.69	0.38	72.3	41.4	3.58	2
129	2002/07/17 17:02	22.00	6	0.17	-8	52	-0.78	$1.9^{+0.1}_{-0.1}$	-16	-8	52	0.48 ± 0.03	8.88 ± 1.99	4.24 ± 1.23	0.28	73.3	37.9	3.75	1
130	2002/12/13 17:02	74.00	2	0.31	25	37	0.63	$-1.4^{+0.2}_{-0.2}$	-11	-13	43	0.39 ± 0.05	6.12 ± 1.47	-2.36 ± 0.86	0.33	76.4	25.2	4.4	2
131	2003/02/12 17:02	43.00	3	0.24	-38	120	0.09	$-1.7^{+0.8}_{-0.8}$	12	-2	67	0.33 ± 0.17	6.73 ± 1.95	-2.20 ± 1.80	0.33	77.3	20.9	4.61	1
132	2004/02/25 19:55	21.00	2	0.16	30	60	0.64	$-0.9^{+0.0}_{-0.0}$	17	1	64	0.24 ± 0.01	3.07 ± 0.75	-0.75 ± 0.20	0.18	81.1	-0.2	5.36	2
133	2004/07/24 19:55	63.00	1	0.43	-23	218	0.83	$0.5^{+0.1}_{-0.1}$	18	4	43	0.49 ± 0.06	3.59 ± 0.91	1.77 ± 0.65	0.47	82.4	-7.7	5.41	2
134	2004/08/23 17:02	79.00	2	0.50	-60	141	0.23	$0.8^{+0.2}_{-0.2}$	7	15	67	0.26 ± 0.35	14.53 ∓ 3.75	18.30 ± 9.81	0.45	82.6	-9.1	5.4	1
135	2004/10/19 21:07	105.00	0	0.41	53	337	-0.27	$0.6^{+0.1}_{-0.1}$	3	-4	56	0.31 ± 0.02	2.36 ± 0.57	0.73 ± 0.23	0.36	83.2	-12.0	5.37	2
136	2005/03/11 09:07	61.00	3	0.28	22	306	-0.37	$1.5^{+0.3}_{-0.3}$	-73	-18	57	0.46 ± 0.11	9.21 ± 2.36	4.23 ± 2.12	0.41	84.6	-19.3	5.22	2
137	2005/05/19 03:07	23.00	4	0.15	60	1	-0.59	$1.1^{+0.1}_{-0.1}$	-3	14	60	0.46 ± 0.02	6.53 ± 1.61	3.01 ± 0.85	0.16	85.4	-23	5.09	1
138	2005/05/22 00:57	88.00	1	1.23	-56	30	-0.92	$0.1^{+0.0}_{-0.0}$	95	-9	61	8.24 ∓ 0.18	8.29 ± 2.32	68.35 ± 20.66	0.37	85.4	-23.2	5.09	2
139	2007/07/04/13:55	20.00	12	0.07	22	225	0.21	$1.9^{+0.3}_{-0.3}$	16	-17	49	0.29 ± 0.02	2.10 ± 0.69	0.62 ± 0.25	0.25	255.8	-26.5	1.48	2

Note. Events 1–19 are from Raghav et al. (2020), 20–92 from Lepping et al. (2006), and 93–139 from Du et al. (2010). Columns 2 and 3 are the start time and duration (in units of hours) of an MC, respectively. Columns 4 to 16 indicate the fitting parameters of our model, which are respectively: the axial magnetic field strength, B_0, the radius of the cross section, R, the elevation angle, θ, the azimuthal angle, ϕ, the closest approach of the observational path to the MC, d, the number of turns per unit length, τ, the expansion speed, v_e, the plasma poloidal speed, v_p, the angle between the MC axis and the Sun–spacecraft line, Θ, the axial magnetic flux, F_z, the poloidal magnetic flux, F_p, the total magnetic helicity, H_m, and the evaluation parameter for good or bad fitting, χ_n. Columns 17–19 indicate the longitude, latitude, and the heliodistance, respectively. Q is the quality of the fit. For the model parameters, B_0 is in units of nT, R in astronomical units, θ, ϕ, and Θ in units of degrees, d in units of R, τ in astronomical units, F_z, F_p in units of Mx and H_m in units of Mx^2.
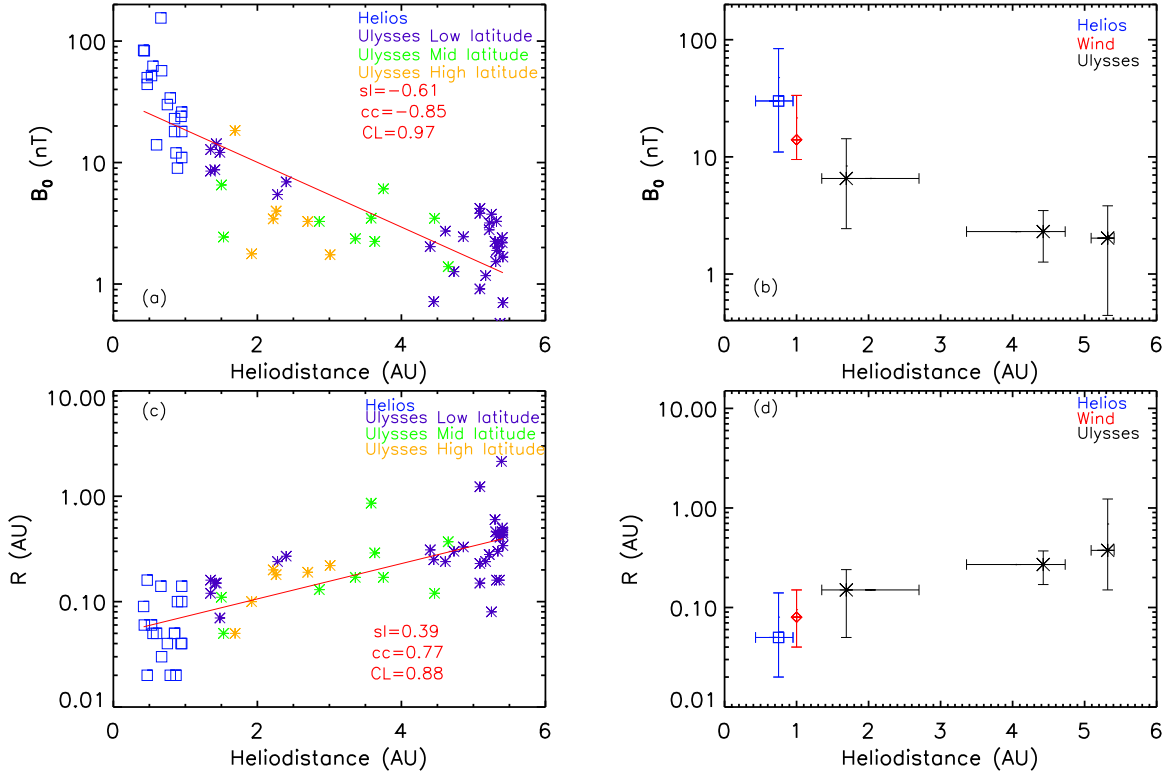
Figure 1. Variation of the axial magnetic field strength (B_0) and the radius of the cross section (R) of the flux rope with heliocentric distance (in au). Panels (a) and (c) are scatter diagrams in which the blue symbols denote the fitting results of MCs observed by Helios, and the purple, green, and yellow symbols denote the fitting results of the MCs at low, middle, and high latitudes observed by Ulysses, respectively. The red lines indicate the linear fitting results. sl, cc, and CL are the slope of linear fitting, the correlation coefficient, and the confidence level by a permutation test, respectively. Panels (b) and (d) are median value diagrams.
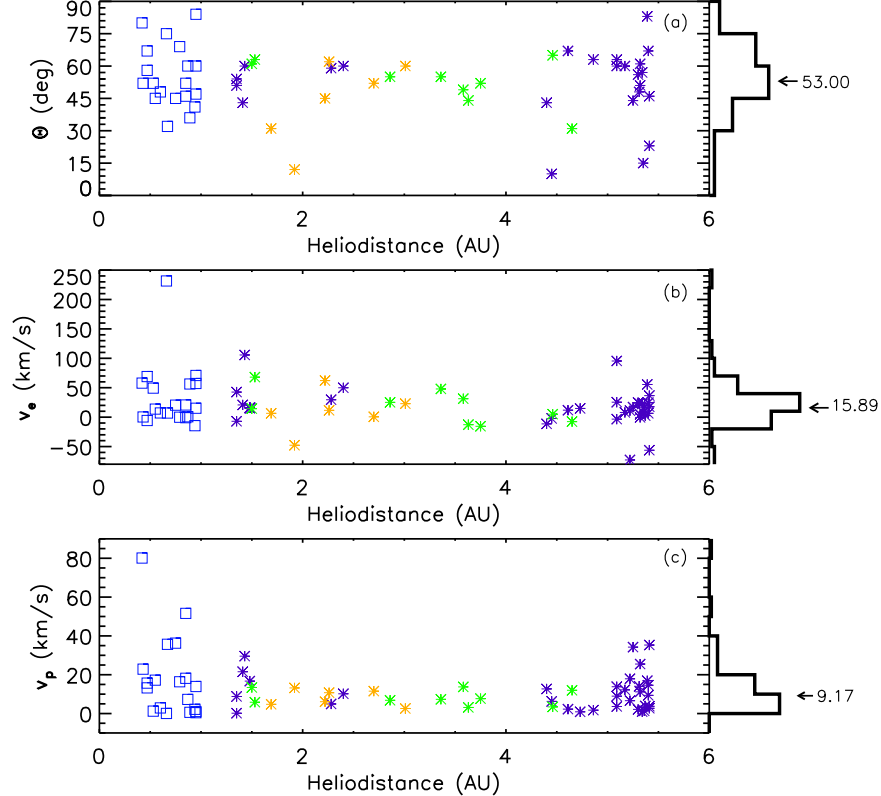
Figure 2. The relationship between Θ, v_e, and v_p and the heliodistance; Θ is the angle between the MC axis and the Sun–spacecraft line, v_e is the expansion speed, and v_p is the poloidal speed. In the three scatter diagrams, the different colored symbols have the same meaning as in Figures 1(a) and (c). The black histograms on the right of the three scatter diagrams show the distribution of Θ, v_e, and v_p. The arrows mark the median values.
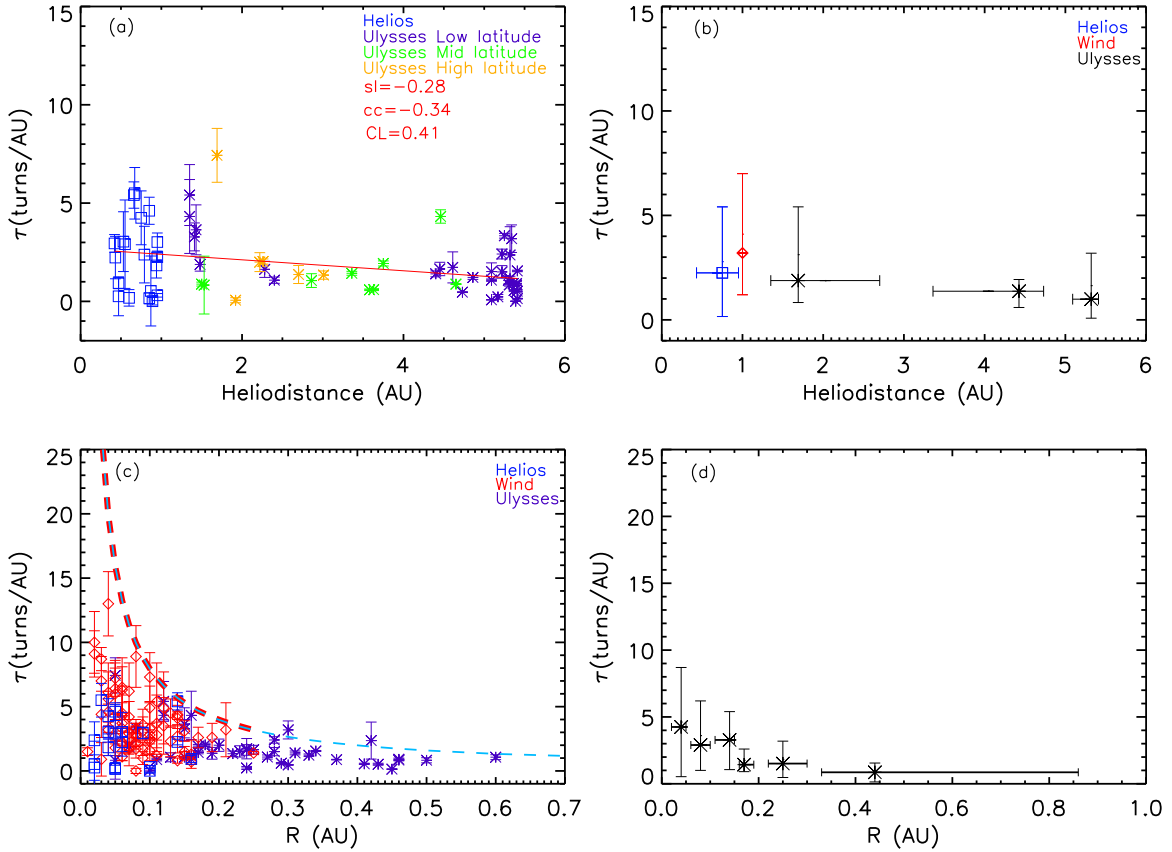
Figure 3. The number of turns of the field lines winding around the axis from one end of the flux rope to the other is plotted vs. the heliodistance in panels (a) and (b) and vs. the radius of the cross section of the flux rope in panels (c) and (d). Panels (a) and (c) show scatter diagrams, and panels (b) and (d) show median value diagrams. In panel (c), the blue, red, and purple symbols denote the fitting parameters of the MCs from the Helios, Wind, and Ulysses spacecraft, respectively. Panel (d) shows the median values and error bars of the MCs at 0–0.05, 0.05–0.1, 0.1–0.15, 0.15–0.2, 0.2–0.3, and 0.3–1 au observed by the Helios, Wind, and Ulysses spacecraft.

from one end of the flux rope to the other is given by

$$n = \tau l. \tag{8}$$

We obtain the median values and error bars of n, F_z, and H_m at 0–0.5, 0.5–1, 1, 1–3, 3–5, and 5–6 au in Figures 4(b), (c), and (f). Figures 4(a) and (b) show the weak positive correlation between n and heliospheric distance, but the tendency to increase almost ceases at 5–5.5 au. Figures 4(d) and (f) show that F_z and H_m decrease within 1 au, after which they remain almost unchanged until 5.5 au, which means that some axial magnetic flux may be converted into azimuthal magnetic flux when the MCs propagate away from the Sun to 1 au.

## 4. Summary and Discussion

In the present study, we investigated the evolution with heliodistance of some parameters from 139 MCs observed by the Helios, Wind, and Ulysses spacecraft. The key findings of the study are:

(1) Clear negative/positive correlations are obtained between the magnetic field strength on the axis/radius of the cross section of the flux rope and the heliodistance; the results are consistent with Leitner et al. (2007).

(2) There are no evident correlations between Θ, v_e, v_p, and the heliodistance. The median values of Θ, v_e, and v_p are

53°, 15.89 km s^{-1}, and 9.17 km s^{-1}, respectively, which means that the spacecraft cross the body of most MCs. In addition, most MCs expand through the inner heliosphere to the outer heliosphere, and plasma poloidal motion is a common phenomenon in MCs.

(3) There is a weak negative correlation between τ and the heliodistance, suggesting that the MCs unwrap when they progress from the inner heliosphere to the outer heliosphere. An evident negative correlation between τ and R shows that thinner flux rope has a bigger twist of the magnetic field lines around its axis.

(4) For a perfectly conducting plasma in a closed volume, the total magnetic helicity is constant. However, the total magnetic helicity in our work appears to decrease within 1 au. It seems that there is a mechanism that translates the axial magnetic flux into azimuthal magnetic flux, possibly because the MC experiences an erosion process (e.g., Dasso et al. 2006; Ruffenach et al. 2012, 2015; Manchester et al. 2014).

In our work, considering the influence of low, middle, and high latitudes on the parameters of MCs, we guess that the parametric properties of the MCs observed by Ulysses on and outside the ecliptic are different because they propagate in two completely different media. The MCs observed at high latitude propagate in a less dense medium that expands at high speed,
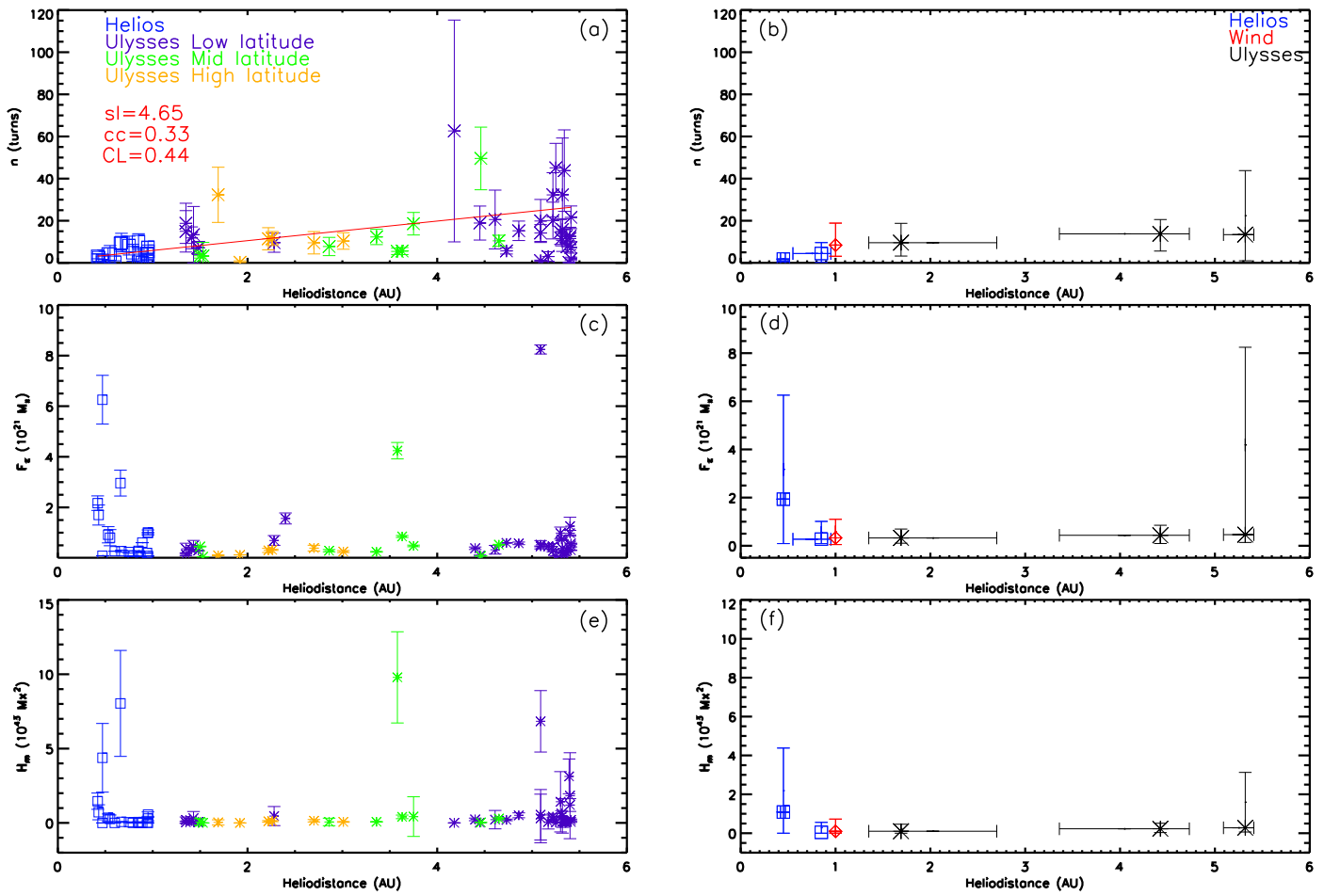
Figure 4. Scatter diagrams of the number of turns of the field lines winding around the axis from one end of the flux rope to the other vs. the heliodistance (a), the axial magnetic flux vs. heliodistance (c), and the total magnetic helicity vs. the heliodistance (e). Panels (b), (d), and (f) show the median diagrams of the above three parameters. The different colored symbols in panels (a), (c), and (e) have the same meaning as those in Figure 1(a).

and MCs observed on the ecliptic undergo significant interaction with at least the Parker spiral-related structures. However, we did not find any evident difference in the parametric properties of MCs on and outside the ecliptic in Figures 1, 2, 3, and 4.

About 32% of MCs cannot be fitted well in our model in the process of filtering data; this may be because the spacecraft does not pass through the center of the MC, or the internal structure of the MC becomes an atypical flux rope structure because it suffers from the interaction between the ambient plasma and the MC during propagation.

ORCID iDs

Ake Zhao ⑩ https://orcid.org/0000-0002-6740-2659
Yuming Wang ⑩ https://orcid.org/0000-0002-8887-3919
Hengqiang Feng ⑩ https://orcid.org/0000-0003-2632-8066
Long Cheng ⑩ https://orcid.org/0000-0003-0578-6244
Qiangwei Cai ⑩ https://orcid.org/0000-0001-5188-0165
Hongbo Li ⑩ https://orcid.org/0000-0001-5649-6066
Guoqing Zhao ⑩ https://orcid.org/0000-0002-1831-1451

References

Burlaga, L., Sittler, E., Mariani, F., & Schwenn, R. 1981, JGR, 86, 6673
Dasso, S., Mandrini, C. H., Démoulin, P., & Luoni, M. L. 2006, A&A, 455, 349
Du, D., Wang, C., & Hu, Q. 2007, JGRA, 112, A09101
Du, D., Zuo, P. B., & Zhang, X. X. 2010, SoPh, 262, 171
Good, S. W., Forsyth, R. J., Eastwood, J. P., & Möstl, C. 2018, SoPh, 293, 52
Good, S. W., Forsyth, R. J., Raines, J. M., et al. 2015, ApJ, 807, 177
Gulisano, A. M., Démoulin, P., Dasso, S., Ruiz, M. E., & Marsch, E. 2010, A&A, 509, A39
Kilpua, E. K. J., Good, S. W., Palmerio, E., et al. 2019, FrASS, 6, 50
Klein, L. W., & Burlaga, L. F. 1982, JGR, 87, 613
Leitner, M., Farrugia, C. J., Möstl, C., et al. 2007, JGRA, 112, A06113
Lepping, R. P., Berdichevsky, D. B., Wu, C. C., et al. 2006, AnGeo, 24, 215
Li, H., Wang, C., Richardson, J. D., & Tu, C. 2017, ApJL, 851, L2
Manchester, W. B., Kozyra, J. U., Lepri, S. T., & Lavraud, B. 2014, JGRA, 119, 5449
Nakwacki, M. S., Dasso, S., Démoulin, P., Mandrini, C. H., & Gulisano, A. M. 2011, A&A, 535, A52
Raghav, A., Gaikwad, S., Wang, Y., et al. 2020, MNRAS, 495, 1566
Rodriguez, L., Zhukov, A. N., Dasso, S., et al. 2008, AnGeo, 26, 213
Ruffenach, A., Lavraud, B., Farrugia, C. J., et al. 2015, JGRA, 120, 43
Ruffenach, A., Lavraud, B., Owens, M. J., et al. 2012, JGRA, 117, A09101
Salman, T. M., Winslow, R. M., & Lugaz, N. 2020, JGRA, 125, e27084
Skoug, R. M., Feldman, W. C., Gosling, J. T., et al. 2000, JGR, 105, 27269
Telloni, D., Zhao, L., Zank, G. P., et al. 2020, ApJL, 905, L12
Vršnak, B., Amerstorfer, T., Dumbović, M., et al. 2019, ApJ, 877, 77
Wang, C., Du, D., & Richardson, J. D. 2005, AGUFM, 2005, SH51C–1230
Wang, Y., Shen, C., Liu, R., et al. 2018, JGRA, 123, 3238
Wang, Y., Zhou, Z., Shen, C., Liu, R., & Wang, S. 2015, JGRA, 120, 1543
Wang, Y., Zhuang, B., Hu, Q., et al. 2016, JGRA, 121, 9316
Witasse, O., Sánchez-Cano, B., Mays, M., et al. 2017, JGRA, 122, 7865